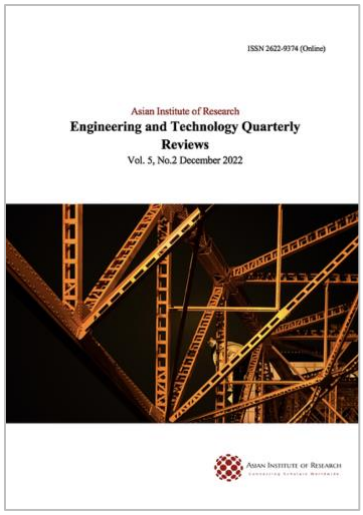


# Engineering and Technology Quarterly Reviews

**Sönmez, A. U., & Vijayan, S. N. (2022), Numerical Analysis of Frictional Drag Reduction of Watercraft Using Water Lubrication Technique. In: *Engineering and Technology Quarterly Reviews*, Vol.5, No.2, 18-29.**

ISSN 2622-9374

The online version of this article can be found at:
**https://www.asianinstituteofresearch.org/**

Published by:
The Asian Institute of Research



The Asian Institute of Research *Engineering and Technology Quarterly Reviews* is a peer-reviewed International Journal. The journal covers scholarly articles in the fields of Engineering and Technology, including (but not limited to) Civil Engineering, Informatics Engineering, Environmental Engineering, Mechanical Engineering, Industrial Engineering, Marine Engineering, Electrical Engineering, Architectural Engineering, Geological Engineering, Mining Engineering, Bioelectronics, Robotics and Automation, Software Engineering, and Technology. As the journal is Open Access, it ensures high visibility and the increase of citations for all research articles published. The *Engineering and Technology Quarterly Reviews* aims to facilitate scholarly work on recent theoretical and practical aspects of Education.

ASIAN INSTITUTE OF RESEARCH
Connecting Scholars Worldwide

The Asian Institute of Research
Engineering and Technology Quarterly Reviews
Vol.5, No.2, 2022: 18-29
ISSN 2622-9374


# Numerical Analysis of Frictional Drag Reduction of Watercraft Using Water Lubrication Technique

Atilla Uygar Sönmez[1], Vijayan S. N.[2]

[1]Department of Mechanical Engineering, Faculty of Engineering, Gaziantep University, Gaziantep, Turkey
[2]Assistant Professor, Department of Mechanical Engineering, Karpagam Institute of Technology, Coimbatore, Tamil Nadu, India.

Correspondence: Atilla Uygar Sönmez. Email: atillasonmez2009@gmail.com

**Abstract**
The majority of the energy expended by watercraft is used to overcome drag. Frictional resistance can account for up to 80 % of overall resistance, especially on large vessels, which leads to an increase the fuel consumption and environmental impacts. As a result, finding strategies to reduce frictional drag is interesting. There are numerous strategies for reducing drag that have already been proposed that are air lubrication techniques, boundary layer energizing, and suction is few of the examples. This study proposes a new way of reducing drag this method is known as water lubrication. To create adverse flow, water jets are used to split the flow. The formation of an auspicious boundary layer ore sluggish boundary layer surrounding the surface it reduces drag significantly. Separation is generally undesired since it expands the wake zone and as a result it produces drags. In flat plate separation it does not significantly enlarge the wake region. Separations form a slow or adversely directed layer on the flat plate if they are created and positioned correctly. This is demonstrated in this study through the use of ANSYS Fluent simulation. Also, with water jet velocities of 3 to 15 m/s drag reductions of 17 % to 134 % have been achieved.

**Keywords:** Watercraft, Friction, Drag Reduction, Water Jet, Flow, ANSYS

## 1. Introduction

When an object moves in a fluid the fluid exerts forces against the object in the flow direction, that force is called Drag. Drag is extremely important for moving objects because it is a force that moving objects must overcome. If a watercraft wants to go speed (V) against drag (D) must have D*V power. The needed power must be proportional to the drag or the required energy is equal to force time distance. Most of the transportation cost comes from drag. Spending higher amounts of energy (fuel) do not only mean losing money but also causes environmental pollution because of carbon emissions from spent fuel. When an object moves through fluids on its surfaces, pressure builds up and shear stresses are distributed. Pressure forces are perpendicular to the surface and friction forces are tangent to the surface.

Total surface integration of these forces gives total acting force (TF). Lift occurs when the flow component of the TF is perpendicular to the flow component, and drag occurs when the flow component of the TF is parallel to the flow component. The forces generated from the fluid are shown in figure 1. The viscous component of the drag is also called skin friction drag because it occurs on the object surfaces. Skin material, roughness, and skin microstructure are quite effects of the viscous drag beside the fluid viscosity. The pressure sourced component of the drag is called form drag or pressure drag.

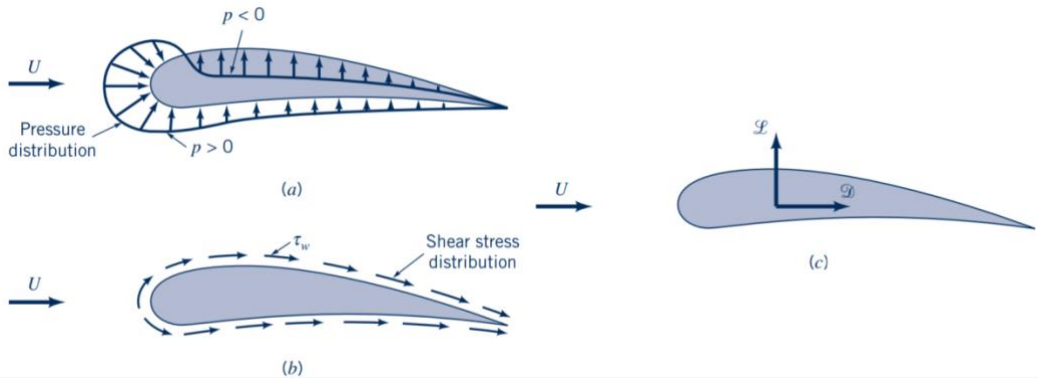


Figure 1: Forces from surrounding fluid (a) pressure force, (b) viscous force and (c) resultant force [1]

Equation (1) and (2) is used to determine the total drag and coefficient of drag. Also, it can be useful to know local shearing stresses and pressure distribution around moving objects. The resultant forces (Drag) can be obtained from the experimental drag coefficient (Cd).

D = Total Drag = Pressure component of drag + Friction component of drag = Dp+Df

$$D = \int dFx = \int PCos\theta dA + \int \tau x Sin\theta dA \quad (1)$$

$$Dp = \int PCos\theta dA$$

$$Df = \int \tau x Sin\theta dA$$

Where $\theta$ is the angle between surface normal and free stream flow direction (x-direction)

$$Cd = \frac{D}{\frac{1\rho U^2 A}{2}} \quad (2)$$

While viscous drag accounts for a larger share of the drag at low Re, pressure drag accounts for a larger portion of the drag at high Re, where inertial forces dominate. Drag is proportional to the square of velocity as shown by the simple formula above. Watercraft required power to overcome drag and it will be proportional to the cube of the velocity. As a result, finding strategies to minimise drag coefficient without compromising velocity is critical. The water lubrication technique uses boundary layer separation to reduce drag. When the boundary layer separates streamlines no longer flow parallel to the object surface and each other. Local shearing stress is zero at the separation zone. There are two basic types of boundary layer separation they are pressure-based and geometry-based separations.

In geometry-based boundary layer separation, when the shape of a moving object changes abruptly or sharp turns on the flow can lead to occur immediate separation at the corner (B) which is shown in figure 2 (b). Fluid cannot follow the object's surface due to inertial forces. If you desire a streamlined object, you should avoid this type of contour. However, sometimes it can be an inevitable boundary layer or be employed for design purposes. For example, cavitation techniques for reducing drag.

Flow around the object transfers kinetic energy into potential energy (as pressure) in pressure-based boundary layer separation, depending on the shape of the object (or vice versa). The exchange occurs without loss in the inviscid flow and does not result in separation. Although there is a boundary layer in an actual flow that causes severe viscosity effects and energy loss. As a result, the conversion of kinetic energy to potential energy is never 100 %. The separation occurs when the flow does not have enough energy to enter the high-pressure area due to actual flow losses. In basic analyses, we can assume the upper boundary of the boundary layer as a streamline to discover pressure distribution as outside the boundary layer inviscid flow equations is valid and inside the

boundary layer, perpendicular pressure gradient is negligible. The pressure distribution on the boundary of the boundary layer becomes pressure distribution inside the boundary layer shelves. The pressure distribution along the object surface is a highly important factor in boundary layer separation. The pressure-based boundary layer separation occurs due to a negative pressure gradient on the surface. Surface pressure rises owing to streamlining expansion in this form of boundary layer separation alongside the object. Pressure-based boundary layers form on gradually longer surfaces as seen in figure 2 (a). When pressure rises, the fluid decelerates and loses energy due to momentum loss in viscous flow. Separation might occur when the flow ultimately comes to a halt.

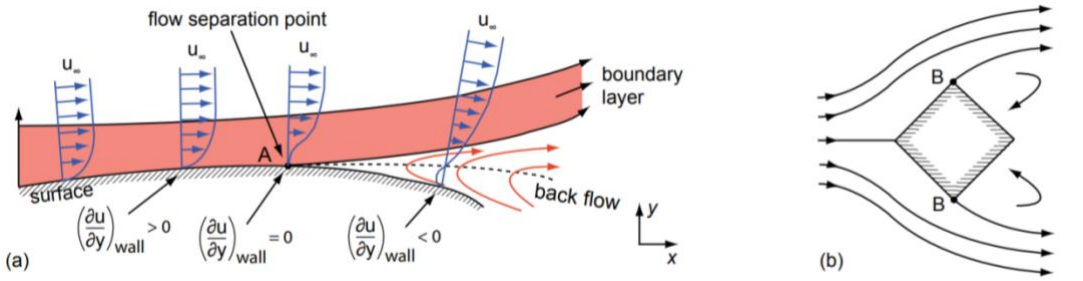


Figure 2: (a) Pressure-based and (b) geometrically-based flow separation [2-4].

The fluid accelerates initially due to a positive pressure gradient (figure 2 (a)). This type of flow is advantageous to the boundary layer since it does not cause separations and tends to maintain laminar flow conditions. The flow speed is constant and fluid acceleration is zero when the pressure gradient is zero. The flow starts to slow down along the streamlines beyond that point $(\frac{\partial P}{\partial x})_{wall}>0$, which could be due to momentum loss or geometry. Separation phenomena require an unfavourable pressure gradient, however, this is insufficient. At the same time, viscous shear stresses demand a long-term retarded fluid so this type of separation does not occur suddenly. The wall first declines and then becomes zero due to the adverse pressure effect in the boundary layer $(\frac{\partial u}{\partial y})$ and u=0 due to the no-slip condition on the wall it appears at a point of stagnation and the flow has begun to divide. Backflow is a fascinating phenomenon that occurs when one flow opposes another. Figure 3 shows the boundary layer velocity distribution before and after the separation of the boundary layer.

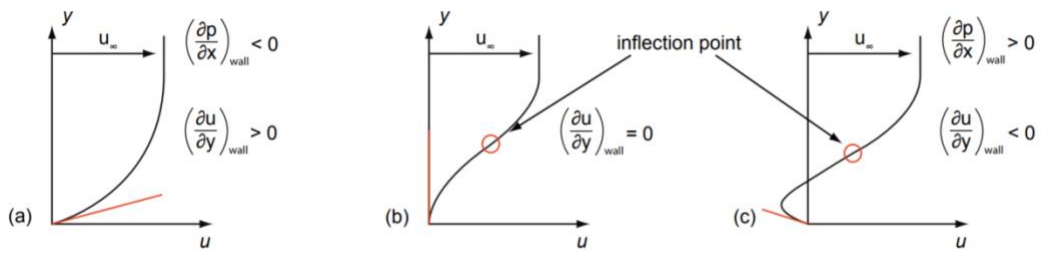


Figure 3: Flow profile of an airfoil (a) before boundary layer separation (b) during boundary layer separation and (c) after boundary layer separation [2].

Figure 3 (a) shows that the separation favours a boundary layer pressure gradient along the flow direction $(\frac{\partial P}{\partial x})_{wall}<0$ indicates that the flow is accelerating and $(\frac{\partial u}{\partial y})_{wall}>0$ indicates that momentum is being transferred along the flow direction and boundary layer. The velocity profile inside the boundary layer is steeper due to the pressure acceleration effect (Shown with a red line). This inclination will steadily decrease until it reaches point b, where it will become zero and then negative after separation (c). Figure 3(b) indicates that there is no shear force on the wall and that the fluid does not move in the x-direction when $(\frac{\partial u}{\partial y})_{wall}=0$. The pressure forces work to decelerate the fluid along the surface when $(\frac{\partial P}{\partial x})_{wall}>0$ which is represented in figure 3(c). Because of the strong vorticity and unpredictable eddies, the boundary layer dissipates after the separation point or line, and the wake zone begins. The turbulent boundary layer and the wake zone are two distinct phenomena. The laminar boundary

layer area may be the starting point for wake and separation. The different types of boundary layer separation are shown in figure 4.

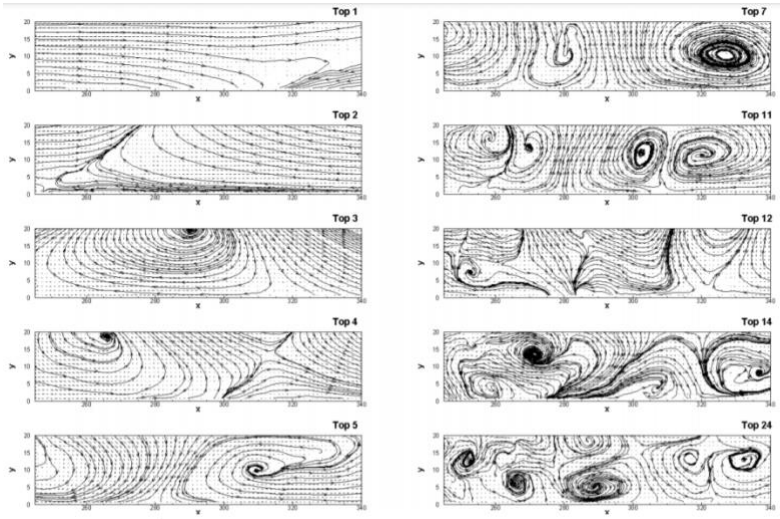


Figure 4: Boundary layer flow separation types [5].

Separated flow can be reattached in its natural nature of flow under certain conditions. When there is a separation in the laminar boundary layer section due to insufficient adverse pressure, the flow may shift to the turbulent boundary layer, where it can reattach due to the higher energy of the turbulent boundary layer flow. The size of the laminar recirculating zone is influenced by initial flow disturbances and the form features of the object. In the studies, the reattached flow had a detrimental impact on flow drag characteristics. Furthermore, there is an unfavorable flow in the recirculating zone, which necessitates a lower or negative frictional drag. The formation of reattachment of separated flow is shown in figure 5.

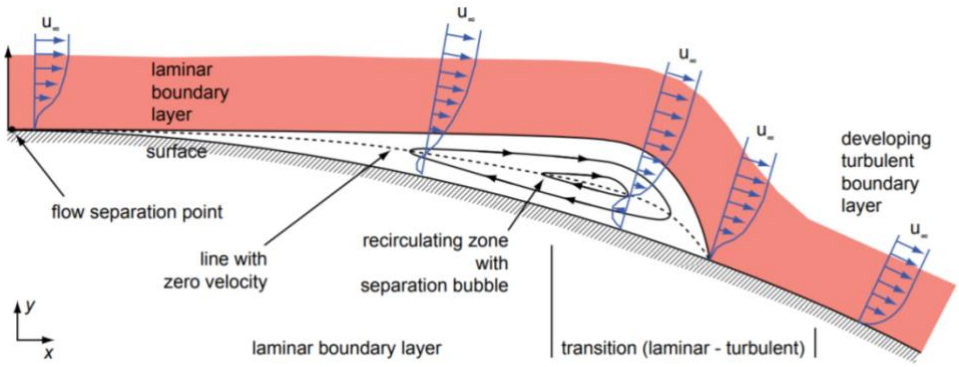


Figure 5: Reattachment of separated flow [6].

**2. Water Lubrication Technique**

The water lubrication technique uses flow separation for drag reduction. Water jets are used to change boundary layers in the water results drag reduction and also the creation of negative drag. Figure 6 depicts the drag (D) and shear stress ($\tau$) gradients created by airflow around a flat plate. As shown in figure 7, the produced friction drag works against the thrusting flow. Shearing stress must be necessary to achieve negative drag as seen in figure 8, after separation the shear forces against the flow direction can be detected.


Figure 6: Expected friction drag and shear stress and their directions on a flat plate


Figure 7:Direction of the drag and shear stress on a flat plate following water lubrication**.**

Water lubrication uses water jets to produce artificial separation points along the surface. Backflow (reverse flow) occurs near a separation point, causing reverse shear stresses, which aid in understanding the water jet lubrication process. On the other hand flat plate separation does not increase the wake region. Water jets from 1 mm holes are predicted to cause separation and reverse flow. This makes sense because surface jets carry adjacent fluids as well as resulting in recirculating zones and reverse shear stress. Water lubrication technique is environmentally friendly and a cheaper solution to reduce frictional drag, transportation cost and emissions.

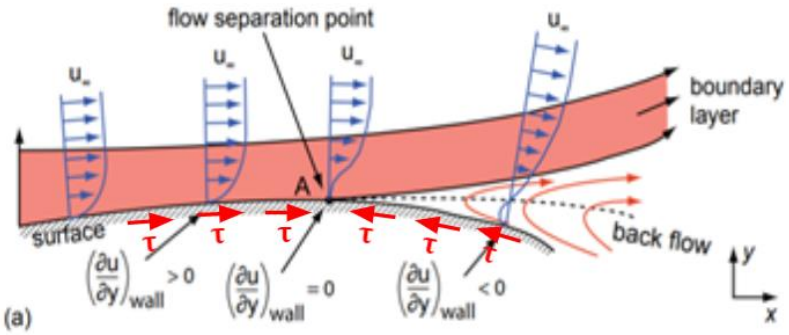


Figure 8: Reverse shear stress and the reverse flow around a separation point

### 3. Literature Review

Drag reduction and boundary layer modification were performed using various drag reduction techniques to decrease the drag force [7-9], such as dielectric barrier discharge plasma actuators for energizing boundary flow and drag reduction [10-11] , also different types of actuators were used to accelerate boundary layer [12]. Another technique to reduce drag is by creating cavitations using water or air [13]. Air lubrication develops and uses a layer near the object's surface that has a far lower average viscosity and density than water. There have been numerous theoretical and experimental investigations have been conducted on the boundary layer created by a fluid jet in order to reduce drag [14].By installing an air lubricating system beneath the ship's hull, air cavities can be exploited to reduce frictional drag. The ship's speed might be enhanced while using air as a lubricant, reducing both fuel consumption and environmental impact. Computational fluid dynamics are used to analyze fluid flow [15]. To conduct numerical analysis fluent software is used, which provides the ability to create and simulate boundary layer with cost-effective and high accuracy. Sometimes numerical analysis may give more accurate results than the real experiment. It gives comprehensive information about simulation prediction for different flow conditions [16-18].Sometimes in the given conditions (flow velocity) turbulent flow delays separation and gives less drag than laminar flow[19-20].These techniques appear to be unattractive to the boundary layer at first glance. When adopting this procedure, rough surfaces produce less drag than smooth surfaces. Another attractive method for reducing frictional drag is air lubrication, which is frequently used in commercial applications and offers favourable and encouraging results [21-24]. The goal of most of drag reduction strategies is to prevent flow separation and reverse flow. However, the water lubrication approach used a water jet to induce flow separation and reverse flow [25-29], [34].

## 4. Numerical Analysis

Before implementing in a real-time application, finite element analysis is used to forecast the reaction of a working component when it is exposed to external loads, fluid flow, heat transfer, and other physical phenomena. The distribution of stress, strain, total deformation, flow velocity, shear stress, and other parameters can be determined by using finite element analysis to analyze the component. We can predict the output values based on these results without having to implement in a real-time application [30-32]. Fluent software is utilized to forecast the percentage of drag reduction when water lubrication is applied. A two-dimensional model of a flat-plate (1000 mm) structure was constructed and evaluated with 9 holes (1mm size) drilled into the flat plate to inject water in the form of a jet between the distance of 100 mm. Figures 9&10 demonstrate the imaginary drag reduction tile and boundary conditions employed in the CFD study. The water jet is injected through the holes in the watercraft's wall into the external surface. The watercraft is surrounded by a high-velocity water flow with a velocity of 8 m/s$^2$.

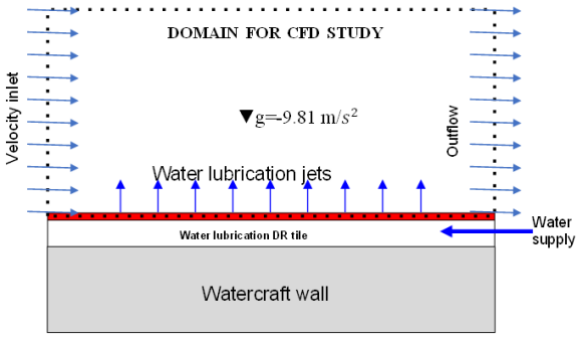


Figure 9:Imaginary drag reduction tile used for water lubrication.

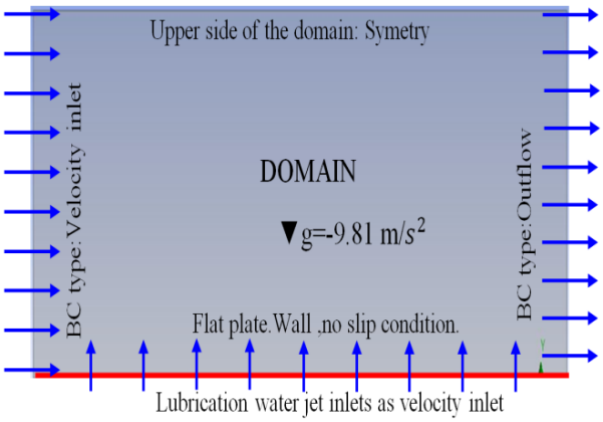


Figure 10:Domain used for CFD study with boundary conditions.

## 5. Mesh independency

| mesh size (k) | drag (N) |
|---|---|
| 19 | 3,42 |
| 35 | -0,6 |
| 65 | -3,5 |
| 88 | -3,9 |
| 114 | -4,4 |
| 161 | -5,33 |
| 207 | -3,35 |
| 394 | -3,58 |
| 447 | -3,57 |

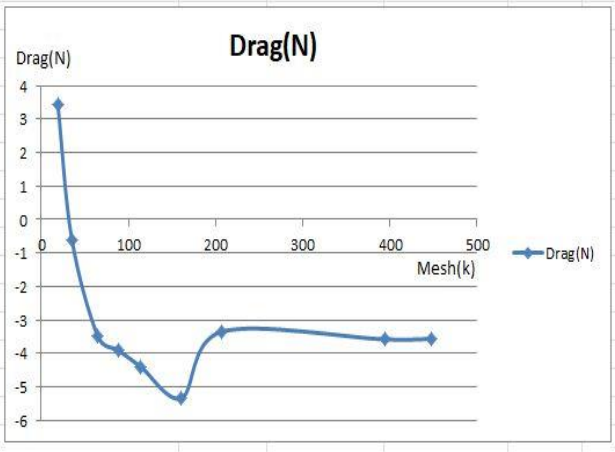


Figure 11: Drag results for different node sizes (12 kg/s airflows).

The analysis was run with various node counts to determine the optimum node count, and the results were analyzed to establish the optimum node count. Figure 11 shows a graph of mesh size and drag achieved with node sizes ranging from 19 k to 447 k. The drag value decreases gradually from 207 k to 447 k nodes and maintains a steady-state condition between 394 k and 447 k nodes. The drag difference between these nodes is roughly 0.3 %. As a result, the analysis was carried out with a node of 447 k which is shown in figure 12.

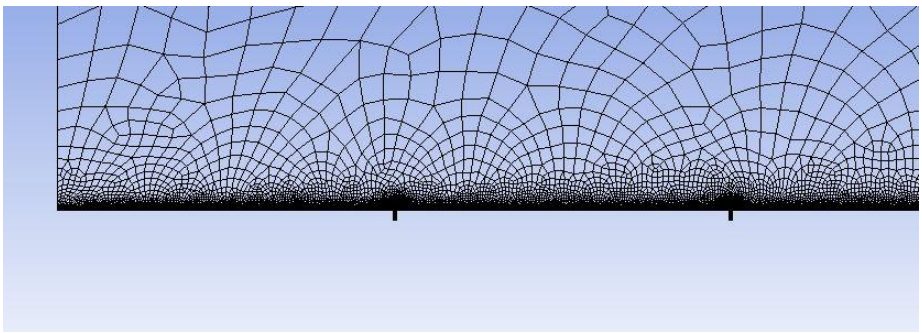

Figure 12: Meshing of the domain for 447k node

The friction drag was calculated using equation (3) as 108.4 N by considering water jet flow (zero), area of the flat plate (1 $m^2$), water flow velocity (8 m/s), water density (998.2 $kg/m^3$) and viscosity (0.001003 kg/m-s).

$$C_f = \frac{\tau_w}{\frac{\rho U^2}{2}} \quad (3)$$

From these values, it can be calculated that Re is 7.96 x$10^6$ which means that flow is the turbulent and the theoretical value of $C_f$ obtained using equation (3) is 3.39 x $10^{-3}$. Figure 13 shows the predetermined value of $C_f$ it is roughly around 3.2 x $10^{-3}$ for smooth plates, also the difference between the outcomes of numerical analysis and theoretical analysis is 6 %.

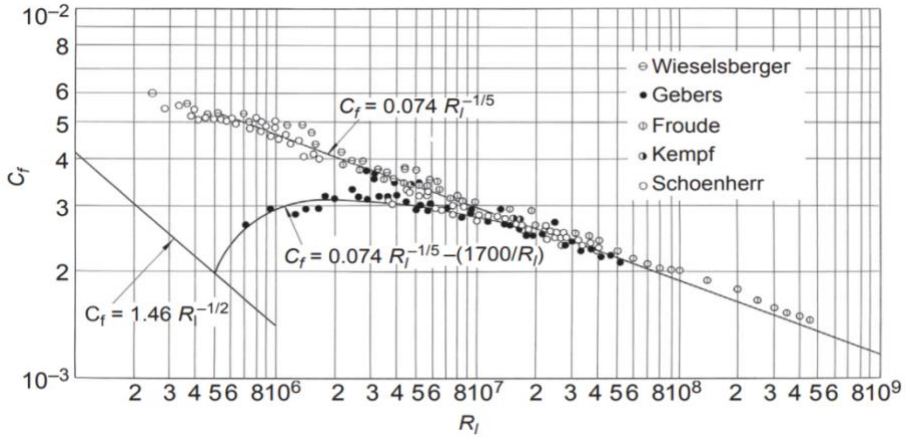


Figure 13:Experimental and theoretical coefficient of friction drag for flat plate [33].

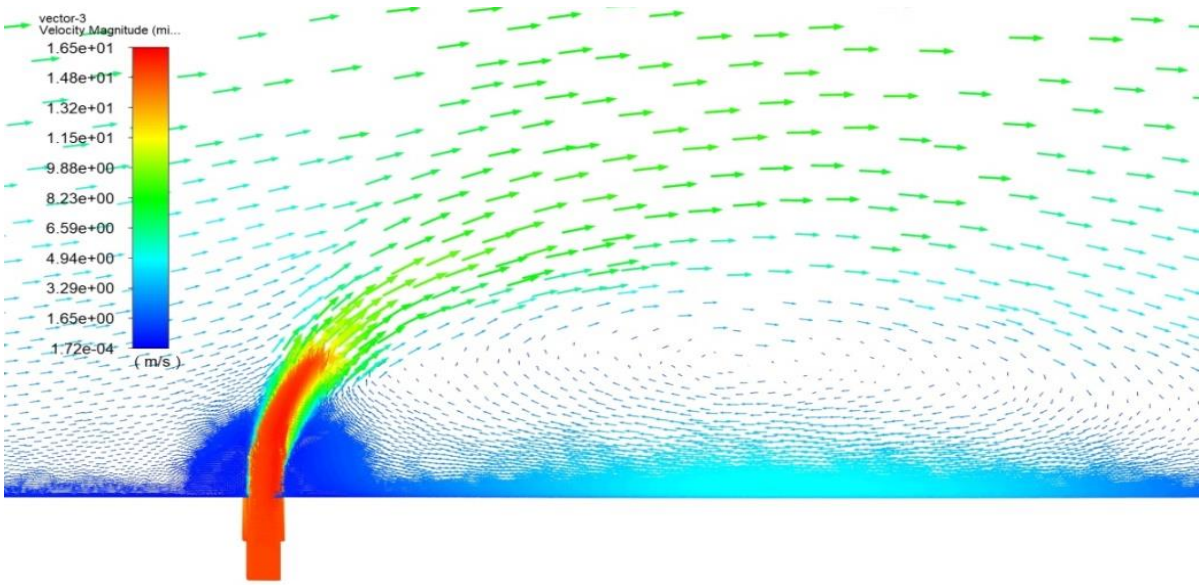


Figure 14: Reverse flows around the water lubrication port.

Figure 14 depicts the formation of a reverse flow (negative drag) and recirculating zone on the rear side of the water jet that is introduced from the watercraft (flat plate). Only one port is zoomed in and exhibited for better understanding. Here, the force exerted by the jet causes the velocity of the flow surrounding it to decrease. Low frictional force can be accomplished by lowering the frictional drag value by reducing the flow velocity between the wall and the water surface. For 1 mm wide slots, a flow output velocity of 12 m/s is necessary to achieve negative drag. Even though reverse flow and drag reduction can be achieved with an output velocity of 3 m/s and strong reverse flows can be created with an output velocity of 4 m/s.

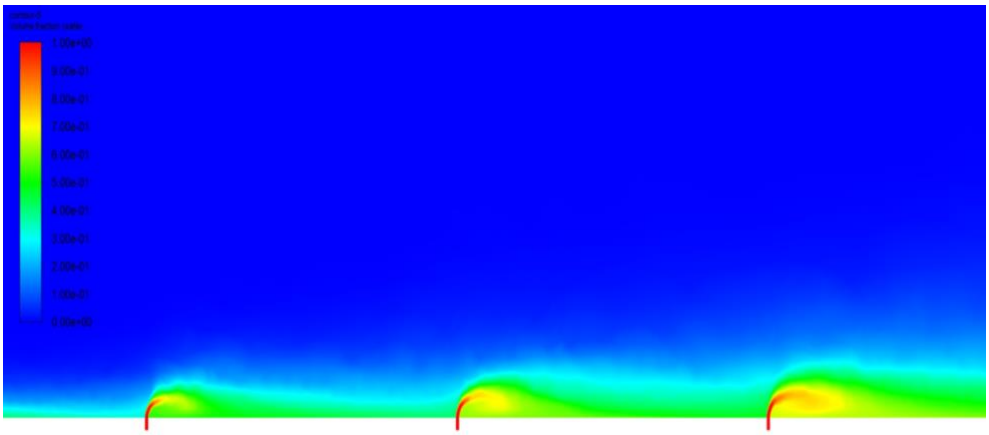

Figure 15: Water jet distributions and their fractions on the domain.

Figure 15 depicts a section of the flow field with three output ports, as well as the effectiveness of water jets. The size and variations of the recirculation zone are depicted in green regions with relation to the jet velocity on the plate, which is gradually raised from the initial water jet location to the last one.

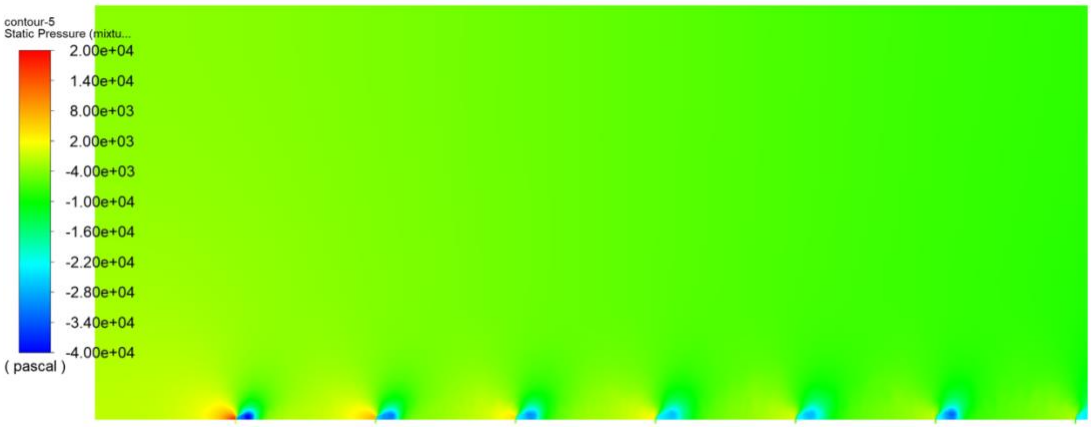


Figure 16:Contours of static pressure.

Figure 16 depicts the pressure distribution before and after the jet, as well as the pressure difference caused. The backward flow is caused by the generated water barrier. Used water can be pulled from the front of the boat, where the high pressure will aid in reducing pressure drag. In addition, when utilised in conjunction with drag reduction strategies, water jets can produce a hollow by acting as a fluid curtain. From the beginning of the water jet port to the end, the developed pressure can be gradually reduced. It is depicted as a blue zone in figure 16.

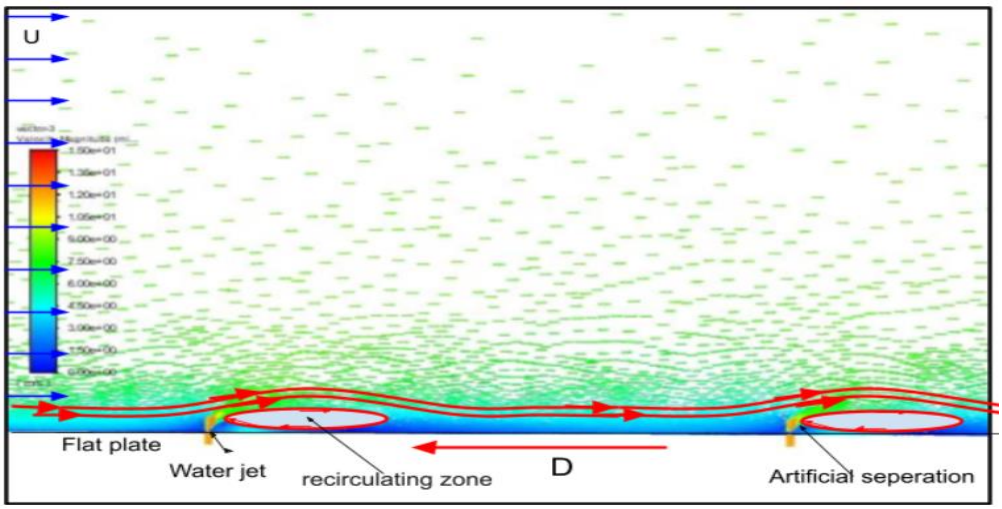


Figure 17: Reverse flow around artificial separation point.

A general view of the flow field during water lubrication is shown in figure 17. Here two water jets are only showcased for discussion purposes (on the plate there are 9). Constantly maintained distances between jets are 100 mm. After injecting water jets into the bottom of the plate the flow is reversed on the plate once the recirculation zones begin which means shear stress is produced against the flow, also the frictional forces thrust the plate against the flow. The flow between the recirculation zones is not reversed, although it is significantly slower. This slow environment on the plate resulted in a slow and thick boundary layer. The velocity of the flow is slowed or reversed as a result of water lubrication in the unique boundary layer, which reduces frictional drag and increases thrust forces.

| Water jet velocity m/s | Calculated drag (N) | DR % | Water jet flux kg/s |
|---|---|---|---|
| 15,00 | -32,88 | 133,7 | 134,8 |
| 12 | -3,99 | 104,1 | 107,8 |
| 9 | 21,05 | 78,4 | 80,8 |
| 6 | 45,78 | 53,1 | 53,9 |
| 3 | 80,13 | 17,9 | 27,0 |
| 0 | 136,5 | -39,9 | 0,0 |

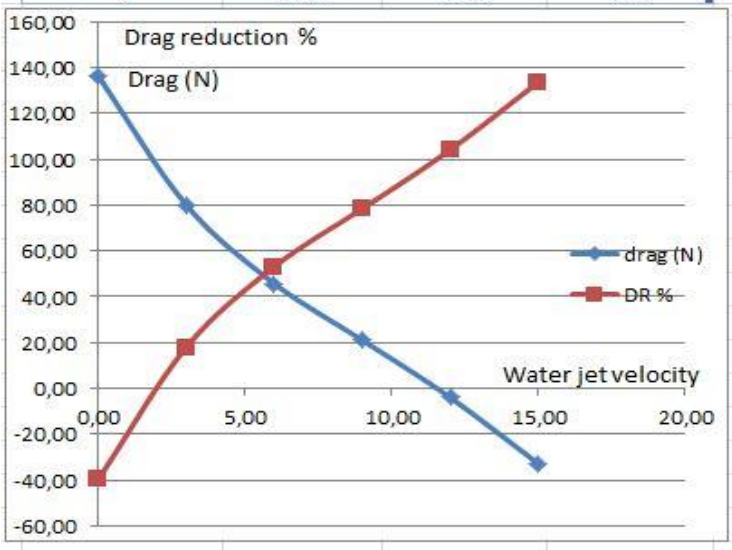


Figure 18: Drag reductions and drags for water jet velocity.

The results of a CFD simulation for a variable water jet velocity are shown in figure 18. In this analysis, the free stream velocity is set at 8 m/s. It is clear from the table and graph is the water jet velocity was increased to 12

m/s, and the percentage of drag reduction climbed to 104% with reducing drag. When the water jet's velocity is increased beyond 12 m/s negative drag is produced which indicates the creation of thrust forces.

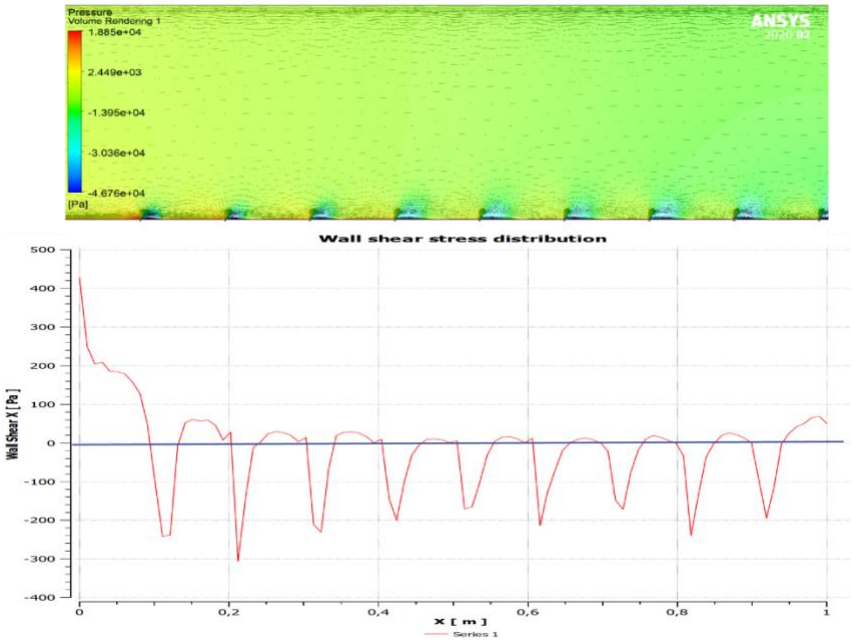


Figure 19: Distribution of wall shear stress

During the flow, shear stress is created owing to friction formed on the wall surface which results in the production of drag force, which varies depending on the shear stress produced on the wall surface. Figure 19 depicts the obtained shear stress distribution of the wall, which clearly illustrates that negative drag force is created in the low shear stress zones. Negative shear stress leads to reduces frictional drag and increases thrust force, which helps to increase the speed of watercraft and also reduces the fuel consumption required to sail the watercraft.

## 6. Conclusion

Separation of flow is an undesirable occurrence as a turbulent flow which is commonly employed to reduce drag by creating turbulence (Turbulent generators). This study has used separation to reduce frictional drag. Using computational fluid dynamics software (CFD), numerical analysis is used to simulate the reduction of drag caused by separating the flow by water jets. In this simulation research, an adverse flow impact was established across the entire surface, resulting in a reverse flow. Continuous changes in drag and shear stress direction can be obtained over the surface during the simulation, which helps reduce frictional drag resistance. As a result of the findings, it was discovered that the slow or adverse flow over the plate generated a separate layer which helps to decrease frictional drag reduction because of its velocity profile. Water is fed in the shape of a jet to the bottom of the watercraft to produce a flow separation and aid in the creation of reverse flow to reduce frictional drag. The CFD results demonstrate a 134 % reduction in friction drag, as well as the possibility of achieving thrust rather than resistance. Furthermore, for a water velocity of 3 m/s, a 17 % reduction in drag can be accomplished. In this study, simulation works only carried out and for better and more accurate results miniature model of the watercraft will be designed and built for testing, optimization and feasibility studies.

## References

Munson, B. R., Okiishi, T. H., Rothmayer, A. P. (2013). *Fluid Mechanics: Fundamentals of Fluid Mechanics (7th Edition)*. John Wiley and Sons Inc: New York.

Sturm, H., Dumstorff, G., Busche, P., Westermann, D., Walter, L., W. (2012). Boundary layer Separation and Reattachment Detection on Airfoils by Thermal Flow Sensors. *Sensors*. 12(11), 14292-306. https://doi.org/10.3390/s121114292.

Schlichting, H., Gersten, K., Krause, E. (2008). *Grenzschicht-Theorie*, 10th ed. Springer Berlin. 377–408. https://doi.org/10.1007/3-540-32985-4.

Bohl, W., Elmendorf, W. (2008). *Technische Stromungslehre*. 14th ed. Vogel-Fachbuch: Wurzburg, Germany, 260–302.

Uruba, V., Knob, M. (2009). Dynamics of a Boundary layer Separation. *Engineering Mechanics*. 16(1), 29–38.

Gad-el Hak, M. (2000). Flow Control-Passive, Active, and Reactive Flow Management, *1st ed.; Cambridge University Press.* Cambridge, UK. 150–203.

David, C. H. (1968). Boundary layer Control. Film Notes. *National Committee for Fluid Mechanics Films.* Princeton University: Princeton.

Craven A. H. (1960). Boundary layers with Suction and Injection A review of published work on skin friction. *Royal Air Force Technical College*, Henlow. http://dspace.lib.cranfield.ac.uk/handle/1826/9420.

Seif, M. S., Tavakoli, M. T. (2004). New Technologies for Reducing Fuel Consumption in Marine Vehicles, *XVI Symposium* SORTA.

Wang, J. J., Choi, K.S., Feng, L. H. (2013). Recent Developments in DBD Plasma Flow Control, *Progress in Aerospace Sciences*. **62**, 52-78. https://doi.org/10.1016/j.paerosci.2013.05.003.

Shimizu, K., Boundary layerajan, M. (2018). Dielectric Barrier Discharge Microplasma Actuator for Flow Control, *Actuators. DOI: 10.5772/intechopen.75802*.

Gerbedon, J.C.,Talbi, A.,Viard, R., Preobrazhenskya, V., Merlenb, A., & Pernod, P. (2015). Elaboration of compact synthetic micro-jets based on micro magneto-mechanical systems for aerodynamic flow control. *Procedia Engineering*. 120, 740 -743. https://doi.org/10.1016/j.proeng.2015.08.789.

Yanga, D., Xiong, Y. L., Guod, X. F. (2017). Drag Reduction of a Rapid Vehicle in Supercavitating Flow. *International Journal of Naval Architecture and Ocean Engineering*. 9(1), 35-44. https://doi.org/10.1016/j.ijnaoe.2016.07.003.

Schlichting, H. (1968). *Boundary-layer Theory*. 6th edition, McGraw-Hill, New York.

Vijayan, S.N., Sendhilkumar., S., Kiran Babu, K. M., Duraimurugan, G.K., & Deepak, P. (2018). CFD Analysis of Frictional Drag Reduction on the Underneath of the Ship's Hull Using Air Lubrication System, *International Journal of Mechanical Engineering and Technology (IJMET).* 9(4), 408–416. https://iaeme.com/Home/article_id/IJMET_09_04_046.

David Paul, D., Vijayan, S.N., Navish Kumar. (2019). Investigation on thermal effects of $Al_2O_3$ Nanoparticles mixed with water in forced convection micro channel using Computational fluid dynamics. *International Journal of Engineering and Advanced Technology*. 8(3),217-222. https://www.ijeat.org/wp-content/uploads/papers/v8i3/C5792028319.pdf.

Kawakita, C., Sato, S., & Okimoto, T. (2015). Application of simulation technology to Mitsubishi air lubrication system. *Mitsubishi Heavy Industries Technical Review*. 52(1), 50-56.

Sililberschmidt, N., Tasker, D., Pappas, T., & Johannesson, J. (2016). Silverstream system - air lubrication performance verification and design development. *Conference of Shipping in Changing Climate*, Newcastle, UK, 10-11.

Merryisha, S., Parvathy, R. (2019). Experimental and CFD Analysis of Surface Modifiers on Aircraft Wing: A Review. *CFD Letters.* 11(10), 46-56. https://akademiabaru.com/submit/index.php/cfdl/article/view/3516.

Spálenský, V., Rozehnal, D. (2017). CFD Simulation of Dimpled Sphere and its Wind Tunnel Verification, *MATEC Web of Conferences.* 107 (1–3), 00077.

McCormick, M. E., Bhattacharyya, R. (1973). Drag reduction of a submersible hull by electrolysis. *Naval Engineering* 85, 11-16. https://doi.org/10.1111/j.1559-3584.1973.tb04788.x.

Yuichi Murai. (2014). Frictional Drag Reduction by Bubble Injection. *Experiments in Fluids*. 55 (1773). https://doi.org/10.1007/s00348-014-1773-x.

Takahashi, T., Kakugawa, A., Nagaya, S., Yanagihara, T., & Kodama, Y. (2001). Mechanisms and scale effects of skin friction reduction by microbubbles. *Proc. 2nd Symp. on the Smart Control of Turbulence*, University of Tokyo, 1–9.

Watanabe, O., Masuko, A., Shirose, Y. (1998). Measurements of Drag Reduction by Microbubbles using very long Ship Models. *Journal of the Society of Naval Architects of Japan*. 183, 53–63. https://doi.org/10.2534/jjasnaoe1968.1998.53.

Ahmed Z. Al-Garni., Abdullah M. Al-Garni., Saad A. Ahmed., & Ahmet Z. Sahin. (2000). Flow Control for an Airfoil with Leading-Edge Rotation. *Journal of Aircraft*. 37(4), 617-622.

Shao, N., Yao, G., Zhang, C., Wang, M. (2017). A New Method to Optimize the Wake Flow of a Vehicle: The Leading Edge Rotating Cylinder. Mathematical Problems in Engineering. 1, 1-16. https://doi.org/10.1155/2017/5781038.

Diamond, P., Harvey, J., Katz, J., Nelson, D., & Steinhardt, P. (1992). Drag Reduction by Polymer Additives. *The MITRE Corporation*, McLean, Virginia.

Wang, J.J., Choi, K.S., Feng, L.H., Jukes, T.N., & Whalley, R.D. (2013). Recent Developments in DBD Plasma Flow Control. *Progress in Aerospace Sciences*. 62, 52-78. 10.1016/j.paerosci.2013.05.003.

Kazuo Shimizu., Marius Blajan. (2018). Dielectric Barrier Discharge Microplasma Actuator for Flow Control. *Actuators*. 10.5772/intechopen.75802.

Vijayan, S. N., Sendhilkumar, S., & Kiran Babu, K. M. (2015). Design and analysis of automotive chassis considering cross-section and material. *International Journal of Current Research*. 7(05), 15697-15701. https://www.journalcra.com/article/design-and-analysis-automotive-chassis-considering-cross-section-and-material.

Singarajan Nagammal Vijayan., Sathiavelu Sendhilkumar. (2015). Structural Analysis of Automotive Chassis Considering Cross-Section and Material. *International Journal of Mechanical Engineering and Automation.* 2(8), 370-376.

Vijayan, S.N., Makeshkumar, M. (2012). Material Specific Product Design Analysis for Conditional Failures – A Case Study. *International Journal of Engineering Science and Technology*. 4(03), 976-984.

Nakayama, Y. (2018). *Introduction to Fluid Mechanics*. 2nd Edition, Butterworth-Heinemann.

Atilla Uygar Sönmez (2022). Water Lubrication for Friction Drag Reduction. *International Scientific Research Congress Dedicated to the 30th Anniversary of Baku Eurasia University,* 1198-1206.

Nomenclatures

| | |
|---|---|
| TF | Total acting force, |
| Cd | Coefficient of drag |
| BL | Boundary layer |
| DR | Drag reduction |
| D | Drag |
| Dp | Pressure drag |
| Df | Friction drag |
| Dw | Wave drag |
| Re | Reynolds number |
| Fr | Froude number |
| PBS | Pressure based separation |
| GBS | Geometry based separation |